JOURNAL OF AGRICULTURAL AND FOOD CHEMISTRY

New Compounds Obtained by Evolution and Oxidation of Malvidin 3-*O*-Glucoside in Ethanolic Medium

NOUR-EDDINE ES-SAFI,*,†,‡ EMMANUELLE MEUDEC,† CLAIRE BOUCHUT,† HELENE FULCRAND,† PAUL-HENRI DUCROT,§ GAËTAN HERBETTE,|| AND VERONIQUE CHEYNIER†

INRA-UMR Sciences pour l'Œnologie, 2 Place Viala, 34060 Montpellier, France, Laboratoire de Chimie Organique et d'Etudes Physico-Chimiques, Pôle de Compétences Pharmacochimie, Ecole Normale Supérieure, B.P 5118 Takaddoum Rabat, Morocco, Unité de Chimie Biologique UMR 206, INRA, Route de Saint-Cyr, 78026 Versailles Cedex, France, and Spectropole, Aix-Marseille Université, Case 511, Faculté de St Jérôme, Avenue Escadrille Normandie Niémen 13397 Marseille Cedex 20, France

Two new colorless phenolic compounds were formed from malvidin 3-*O*-glucoside incubated in an ethanolic solution. Their structures were characterized by means of one- and two-dimensional NMR analysis and through electrospray ionization−mass spectrometry. As compared to the structure of the initial anthocyanin skeleton, the first new compound showed the presence of two fused five-membered rings replacing the pyran ring and of a carbonyl function on the 2-position. The first five-membered ring was shown to result from the formation of a new linkage between the B ring 6′-position and the C ring 4-position, while the second was a dihydro furan ring with an oxygenated ether linkage between the 8a-position and the 3-position. The second isolated compound was shown to have similar structure with an ethyl ether moiety in the 3-position instead of the glucose moiety. A mechanism explaining the formation of the isolated compounds involving the passage through the chalcone form of the anthocyanin and an oxidation process is proposed.

KEYWORDS: Polyphenols; anthocyanins; malvidin 3-*O*-glucoside; reaction; product characterization; mass spectrometry; NMR

INTRODUCTION

Anthocyanins constitute a large family of polyphenols widespread in the plant kingdom (*1, 2*), well-known to be responsible for most of the red, blue, and purple colors of fruits, vegetables, and other plant products. They are also widely found in the human diet. These water-soluble pigments are of interest for the food industry because of their potential applications as natural colorants. Anthocyanins have also been discussed in relation to a wide range of biological activities such as improvement of vision (*3, 4*), prevention of cancer (*5–7*), and antioxidant activity (*8–12*).

Among the problems usually encountered in the field of anthocyanin chemistry, their relatively poor stability constitutes one of the main drawbacks for their use as food colorants. Indeed, anthocyanins are very reactive compounds, due to the acidic character of their hydroxy groups and the nucleophilic and/or electrophilic properties of their chemical skeleton (A-ring). While they are stable in intact flowers and fruits due to copigmentation mechanisms (*13*), they show a propensity to color degradation when they are extracted, when plant tissues are disrupted, or generally once removed from their native environment. Several authors have studied the effect of various factors, such as temperature, pH, oxygen, enzymes, metallic ions, ascorbic acid, and sulfur dioxide on anthocyanins stability during processing (*14–22*).

Anthocyanins have been investigated in aqueous solution and have been shown to exist in different forms in equilibrium depending on the pH (*23–25*). Under very weak acidic conditions, four anthocyanin structural types exist in equilibrium as illustrated in **Figure 1** with malvidin 3-*O*-glucoside as an example. In very acidic aqueous solutions, anthocyanins occur as red flavylium cations AH^+. In aqueous media, increasing the pH leads to a reduction of color intensity because of a decrease in the concentration of the flavylium cation AH^+ that is converted into its colorless hemiketal form B through nucleophilic attack of water. This pseudobase form is in equilibrium with the colorless hydroxy chalcone form C. At

* To whom correspondence should be addressed. Tel: +212 37 75 22 61. Fax: +212 37 75 00 47. E-mail: nouressafi@yahoo.fr.
† INRA-UMR Sciences pour l'Œnologie.
‡ Ecole Normale Supérieure.
§ INRA Unité de Chimie Biologique.
|| Aix-Marseille Université.

10.1021/jf8001872 CCC: $40.75
Published on Web 05/23/2008

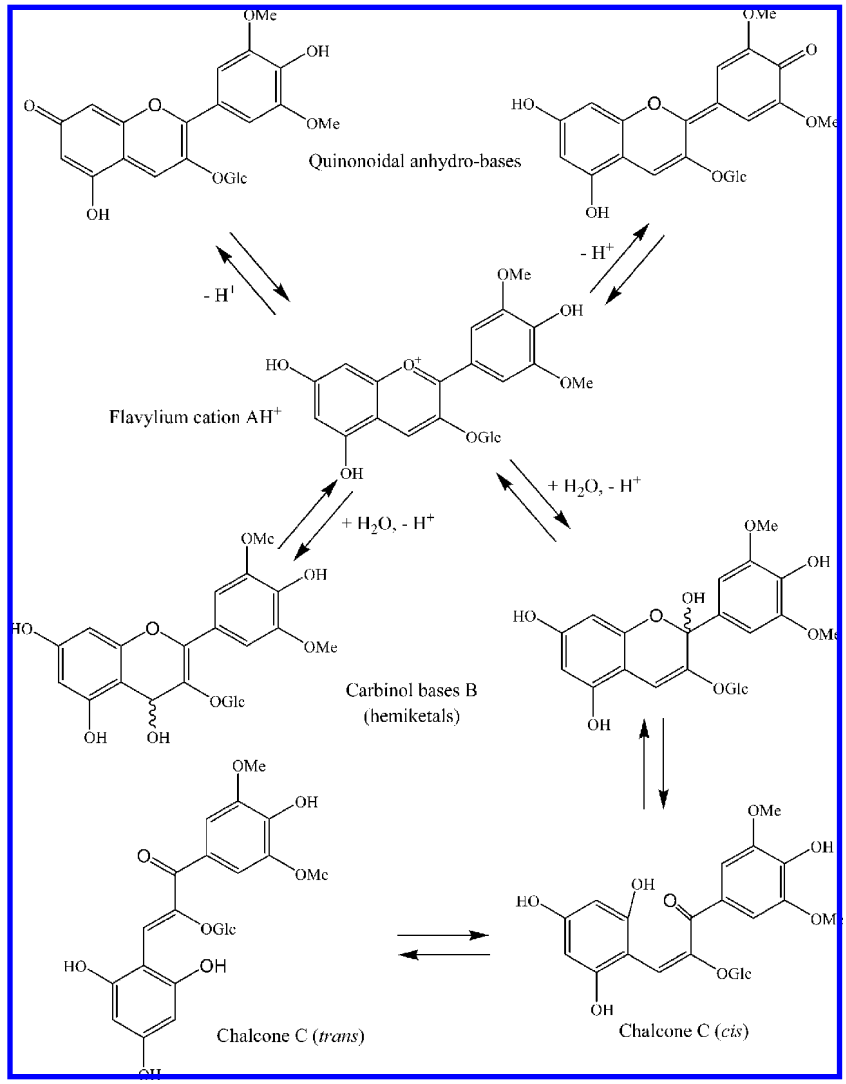

Figure 1. Malvidin 3-*O*-glucoside equilibria in aqueous media (*23*).

low acidic, neutral, and basic pH values, deprotonation of the flavylium cation also occurs, giving rise to the violet/blue quinonoidal forms, although this reaction is very limited in aqueous solutions. It has also been found that, on heating, the equilibrium is driven toward the chalcone form C with a resultant loss in color (*1, 26*).

In addition to these structural changes, the reactivity of anthocyanins has been widely explored especially in relation to wine color changes. Indeed, anthocyanins, which are the red grape pigments and responsible for the color of young red wines, are slowly converted not only into new pigments but also into new colorless compounds. Various processes have been considered to explain these transformations. Studies conducted on model solutions propose different mechanisms such as direct condensation and cycloaddition involving anthocyanins and other compounds like flavanols, quinones, aldehydes, vinylphenols, pyruvic acid, and vinylflavanols that could participate in the formation of these new colored and colorless products (*27–34*).

Noteworthy, the formation of various other compounds of unknown structure has been observed in model solutions (*30*). The structural characterization of these compounds could provide important information regarding the chemical transformations involved in the changes of color during red wine aging. This prompted us to initiate a program aimed at exploring, under different conditions, the transformation of malvidin 3-*O*-glucoside, which is the most encountered anthocyanin pigment especially in grape and derived products. In this study, we investigated chemical changes by reaction of an ethanolic solution of malvidin 3-*O*-glucoside and the structural characterization of two newly formed compounds through two-dimensional (2D) NMR and mass spectrometry.

MATERIALS AND METHODS

Materials. Malvidin 3-*O*-glucoside was isolated from a grape anthocyanin extract from skins of *Vitis vinifera* as described by Sarni et al. (*35*). The crude extract was purified by chromatography on Polyclar SB 100 (DBH Laboratory Supplies, Poole England). After removal of sugars by washing with water/hydrochloric acid (99:1, v/v), malvidin 3-*O*-glucoside was eluted with methanol/water/hydrochloric acid (70:29:1, v/v/v). The anthocyanin purity was controlled by high-performance liquid chromatography coupled to diode array detection and mass spectrometry (HPLC-DAD/MS). Acetonitrile and methanol (HPLC grade) were purchased from Merck (Darmstadt, Germany), and formic acid, acetic acid, and ethanol were purchased from Prolabo (Fontenay s/Bois, France).

Preparation of Solutions. The reaction mixture used consisted of malvidin 3-*O*-glucoside (4 mM) in 30 mL of ethanol. The mixture was purged with argon and maintained at 40 °C in a tube sealed with a Teflon septum. Samples (100 μL) were taken each day by puncturing through the septum and were diluted 10-fold in water/formic acid (95:5, v/v) before analysis.

HPLC-DAD Analysis. HPLC-DAD analyses were performed using a Waters 2690 system equipped with an autosampler system, a Waters

996 photodiode array detector, and Millenium 32 chromatography manager software (Milford, MA). Separation was achieved on a 250 mm × 2.2 mm i.d., 5 μm, 100-RP18 Lichrospher column protected with a guard column of the same material (Merck). The elution conditions were as follows: 0.25 mL/min flow rate; oven temperature, 30 °C; solvent A, water/formic acid (95:5, v/v); and solvent B, acetonitrile/solvent A (80/20, v/v). Elution began isocratically with 2% B for 7 min and was continued with linear gradients from 2 to 20% B in 15 min, from 20 to 30% B in 8 min, from 30 to 40% B in 10 min, from 40 to 50% B in 5 min, and from 50 to 80% B in 5 min, followed by washing and re-equilibrating of the column. UV/vis detection was recorded from 280−520 nm.

HPLC-DAD-Electrospray Ionization (ESI)/MS Analysis. MS experiments and fragmentation analyses were performed on a ThermoFinnigan LCQ Advantage (San Jose, CA) MS equipped with an ESI source and an ion trap mass analyzer, which were controlled by the LCA navigator software. The mass spectrometer was operated in the positive/negative ion mode in the range of *m/z* 250−2000 and under the following conditions: source voltage, 4.5 kV; capillary voltage, 23.5 V; capillary temperature, 250 °C; and collision energy for fragmentation, 25% for MS^2 and 30% for MS^3. Chromatographic separation was achieved using a Waters 2690 system equipped with an autosampler system, a Waters 996 photodiode array detector, and Millenium 32 chromatography manager software. Separation was achieved under the same conditions as for HPLC-DAD analysis.

High resolution MS spectra were obtained on an AccuTOF (JEOL, Tokyo) mass spectrometer equipped with an ESI source and a time-of-flight (TOF) mass analyzer. The spectra were recorded in the negative ion mode, over the range 240−660 Da (needle voltage, −2 kV; orifice voltage, −80 V; and temperature, 300 °C) . Mass center software was used for analysis. Analytes were introduced in LC-MS, and reference standards were introduced by infusion as solutions in methanol. Accurate masses were determined within an error range of 2.27 ppm using a TFA solution as a reference standard. HRMS obtained for compound **1** gave 507.11271 (calcd for $C_{23}H_{23}O_{13}$, $[M - H]^-$, 507.11387).

HPLC/NMR Analysis. Analyses were achieved on compounds isolated through HPLC and solubilized in 1 mL of water/formic acid (98:2, v/v). HPLC analyses were performed on an Agilent 1100 Series (Agilent, Palo Alto, CA) equipped with a quaternary HPLC pump, a degasser, a column heater, and a UV/vis detector and with a refrigerated fraction collector BPSU-36 (Bruker Peak Sampling Unit) interface. Data acquisition and processing were performed using a Bruker Hystar version 2.3 software. Separation was achieved under the same conditions as for HPLC-DAD analysis.

NMR analyses were performed on a Bruker Avance DRX-500 (magnet of 11.75 T) spectrometer equipped with a 5 mm TXI triple resonance inverse cryoprobe with a *z*-axis gradient at 300 K. Samples were solubilized in 50 μL of DMSO-d_6/TFA (9:1, v/v) and poured into a 1.7 mm NMR capillary tube for analysis. Solvent signals (^1H, 2.50 ppm; and ^{13}C, 39.52 ppm) were used as internal standards. ^1H, correlation spectroscopy (COSY), total correlation spectroscopy (TOCSY), heteronuclear multiple-quantum coherence (HMQC), and heteronuclear multiple-bond correlation (HMBC) NMR spectra were acquired using *zg* (*zgpr*), *cosygp*, *mlevgptp*, *inv4gp*, and *hmbc-tango* sequences, respectively.

RESULTS AND DISCUSSION

Transformation of Malvidin 3-*O*-Glucoside and Formation of New Compounds. The solution of malvidin 3-*O*-glucoside in ethanol was incubated at 40 °C and was analyzed each day from the beginning of incubation by LC-DAD/ESI-MS. A progressive decrease in the concentration of malvidin 3-*O*-glucoside was observed. This was concomitant with the formation of new compounds initially absent from the mixture. An example of the obtained chromatographic HPLC profile showing the newly formed compounds is given in **Figure 2**.

Among the major formed derivatives, a first new compound **1** eluting before malvidin 3-*O*-glucoside and having an absorbance maximum between 295 and 330 nm was observed. It may be noted that a compound with similar spectroscopic data had already been detected in our laboratory in a model solution containing (−)-epicatechin and malvidin 3-*O*-glucoside but had not been structurally elucidated (*30*). Another compound **2** showing similar UV/vis characteristics and eluting after malvidin 3-*O*-glucoside was also observed.

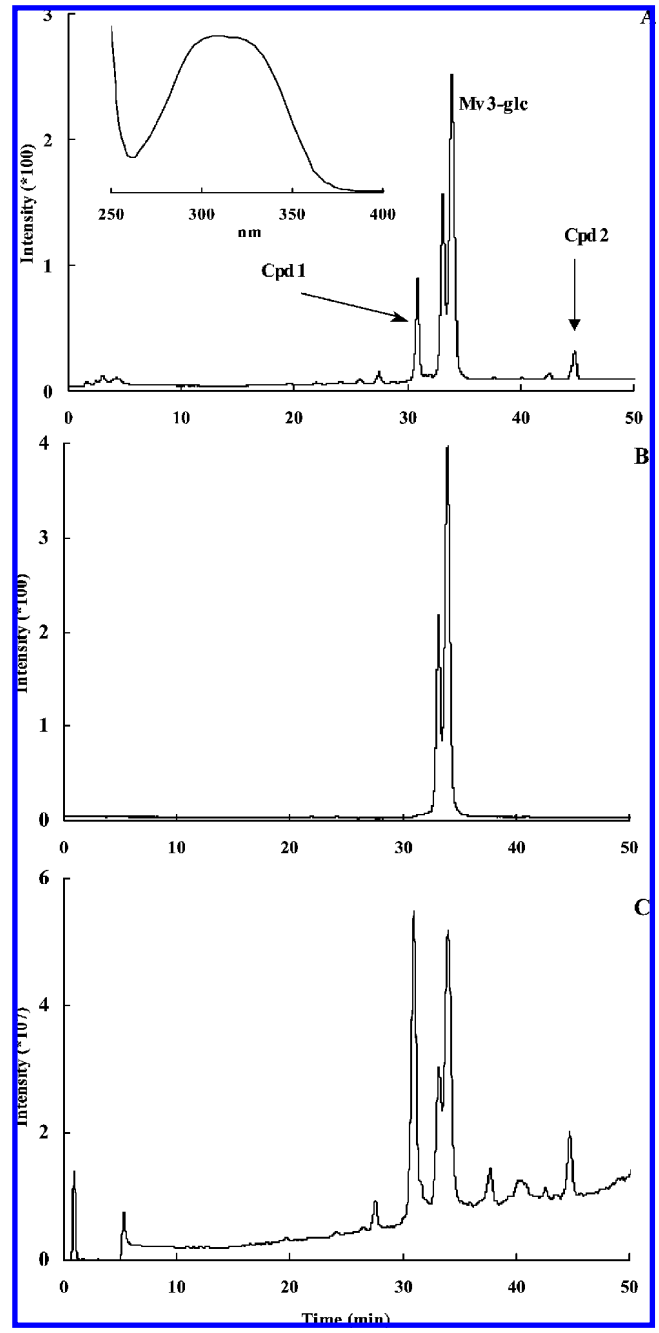

Figure 2. HPLC chromatographic profile recorded at 280 (**A**) and 520 nm (**B**) and with MS (**C**) detection (TIC) showing residual malvidin 3-*O*-glucoside and the newly formed compounds **1** and **2**. The UV spectrum of compound **1** is also shown.

HPLC-ESI/MS analysis of the mixture, conducted in the negative ion mode, showed for compound **1** a mass signal at *m/z* 507 corresponding to the $[M - H]^-$ ion in agreement with a molecular mass of 508 Da. This corresponds to a mass difference of 16 Da as compared to the initial anthocyanin in its flavylium form and of 2 Da as compared to the hemiketal and chalcone forms. Among the fragmentations, the loss of an anhydroglucose moiety was observed at *m/z* 345 ([M − H −

Table 1. ^{1}H and ^{13}C NMR Data of Compound **1** (DMSO-d_6/TFA)

position	δ ^{1}H (ppm), l, m, J (Hz)[a]	δ ^{13}C (ppm)[b]
2		193.1
3		111.5
4	5.27, 1, s	45.6
4a		103.7
5		154.7*
6	5.87, 1, d (1.7)	97.5
7		160.0*
8	5.81, 1, d (1.7)	89.7
8a		160.3*
1′		139.8
2′	7.07, 1, s	102.9
3′		151.1
4′		148.6
5′		143.4
6′		123.5
7′	3.89, 3, s	61.0
8′	3.83, 3, s	56.3
1″	4.49, 1, d (7.8)	98.7
2″	3.05, 1, t (8.1)	73.6
3″	3.11, 1, m	77.5
4″	3.11, 1, m	69.8
5″	2.86, 1, m	77.6
6″a	3.60, 1, dd (12.0, 2.0)	60.8
6″b	3.39, 1, dd (12.0, 5.0)	60.8

[a] Assignments were based on ^{1}H−^{1}H COSY and TOCSY experiments and comparison with literature data. Values were recorded at 500 MHz. Integration: s, singlet; d, doublet; t, triplet; dd, double−doublet; and m, multiplet (J in Hz). [b] Assignments were based on ^{1}H−^{13}C HMQC and HMBC experiments and comparison with literature data. Entries with asterisks could be inverted.

162]$^-$) in addition to the further loss of a water molecule giving a fragment signal at m/z 327 ([M − H − 180]$^-$). This was also confirmed when the analysis was conducted in the positive ion mode where a signal was observed at m/z 531 corresponding to the [M + Na]$^+$ ion.

NMR Analysis of Compound 1. Isolation of compound **1** was achieved by HPLC followed by a complete NMR analysis. A total of six successive injections were done with injected volume going from 5 to 100 μL. The fractions corresponding to the peak **1** were collected, and its structure was determined through spectroscopic analysis. The complete structure of compound **1** was elucidated by ^{1}H and ^{13}C NMR spectroscopy using one-dimensional (1D) and 2D homo- and heteronuclear techniques (COSY, TOCSY, HMQC, and HMBC) (**Table 1**). The chemical structure of malvidin 3-*O*-glucoside along with the numbering used is given in **Figure 3**.

In the ^{1}H NMR spectrum of compound **1**, the presence of the sugar moiety was confirmed by the observation of a signal appearing as a doublet at 4.49 ppm with a large coupling constant (J = 7.8 Hz) characteristic of a β configuration of the sugar moiety and corresponding to the H-1″ proton. The other sugar oxymethine protons were easily assigned through COSY experiment. Thus, the proton H-2″ was attributed to the signal located at 3.05 ppm from its correlation with the H-1″ anomeric proton and the H-3″ proton was attributed to the signal located at 3.11 ppm from its correlation with the H-2″ proton. Following the same reasoning and using the data obtained in the COSY spectrum, the H-4″ and H-5″ protons were attributed to the signals located, respectively, at 3.11 and 2.86 ppm. Finally, the H-6″ protons were assigned to the two sets of double−doublets resonating at 3.60 ppm (J = 12.0 and 2.0 Hz, H-6″a) and 3.39 ppm (J = 12.0 and 5.0 Hz, H-6″b). The multiplicity, the coupling constants, and in addition the observed chemical shifts were all in agreement with a β-D-glucopyranosyl moiety.

The ^{1}H NMR spectrum also showed two singlet signals resonating at 3.83 (H-8′) and 3.89 ppm (H-7′), integrating for three protons each and corresponding to the two B ring methoxy groups. The fact that two distinct signals were obtained indicated that the two methoxy groups were not magnetically equivalent and prompted us to conclude that the symmetry of the initial malvidin 3-*O*-glucoside B ring is disrupted in compound **1**.

In addition to these protons, the ^{1}H NMR spectrum of compound **1** showed four other signals accounting for one proton each and appearing as two doublets at 5.81 and 5.87 ppm and two singlets at 5.27 and 7.07 ppm. The two shielded doublet signals with a low coupling constant (J = 1.7 Hz) were assigned to the two A ring H-6 and H-8 protons as confirmed from the coupling constant value, which is characteristic of an aromatic *meta*-substitution. The singlet at 7.07 ppm, corresponding to an aromatic proton, was assigned to the H-2′ B ring proton. As compared to the B ring of the initial malvidin 3-*O*-glucoside, the second proton was not observed, indicating that the corresponding carbon atom (C-6′) was involved in a substitution. This result also justifies why the methoxy groups gave different signals due to their distinct chemical environments. In the TOCSY spectra, a correlation was observed between the residual proton H-2′ (7.07 ppm) and the methoxy protons (H-8′) located at 3.83 ppm, suggesting that proton H-2′ was in α-position of the methoxy group (^5J) in the aromatic ring. Furthermore, the second methoxy protons (H-7′) located at 3.89 ppm did not show any correlation with the aromatic proton H-2′ located at 7.07 ppm, suggesting a *para*-position of these substituent (^7J). Finally, the ^{1}H NMR spectrum showed a singlet signal at 5.27 ppm. In the TOCSY spectra, this proton signal showed cross-peak correlations with the methoxy protons H-7′ located at 3.89 ppm. This indicates that the proton located at 5.27 ppm is linked to a carbon atom, which is itself linked to the C-6′ carbon.

In the HMQC spectrum, correlations were observed between each proton and the corresponding carbon atoms, allowing us to attribute their respective chemical shifts. Thus, the signals located at 97.5 and 89.7 ppm were easily assigned to the C-6 and C-8 atoms. The chemical shifts of the glucopyranosyl moiety carbon atoms were attributed to the signals located at 60.8 (C-6″), 69.8 (C-4″), 73.6 (C-2″), 77.5 (C-3″), 77.6 (C-5″), and 98.7 ppm (C-1″). The ^{13}C NMR chemical shift of the carbon atom (C-1″) linked to the anomeric proton showed that it was involved in the *O*-glucosidic bond with the aglycone moiety.

The protons of the two methoxy groups showed correlations ^1J with two distinct signals located at 61.0 ppm (C-7′) and 56.3 ppm (C-8′) corresponding to the two methoxy carbons. Generally, a methoxy substituent on an aromatic system lies in the plane of the ring. In such a conformation, there is the maximum overlap between the lone pair of the oxygen and the π-orbitals of the aromatic ring. The low deshielding observed in the ^{13}C NMR signal (+5 ppm) of the C-7′ methoxy carbon as compared to the C-8′ methoxy carbon could be due to a less extended conjugation of the lone pair of the oxygen C-7′ methoxy with the aromatic ring as compared to the lone pair of the oxygen C-8′ methoxy (*36*). This fact is in agreement with the presence of a substitution on the adjacent carbon atom, C-6′.

The aromatic proton H-2′ located at 7.07 ppm gave in the HMQC spectrum a correlation with a signal located at 102.9 ppm (C-2′) confirming its aromatic nature. Finally, a cross-peak correlation was observed between the singlet signal proton observed at 5.27 ppm and the carbon signal located at 45.6 ppm, indicating its sp^3 nature. This carbon atom was thus concluded to be of a tertiary nature having a proton as a substituent and being linked to the C-6′ B ring carbon atom. The fourth

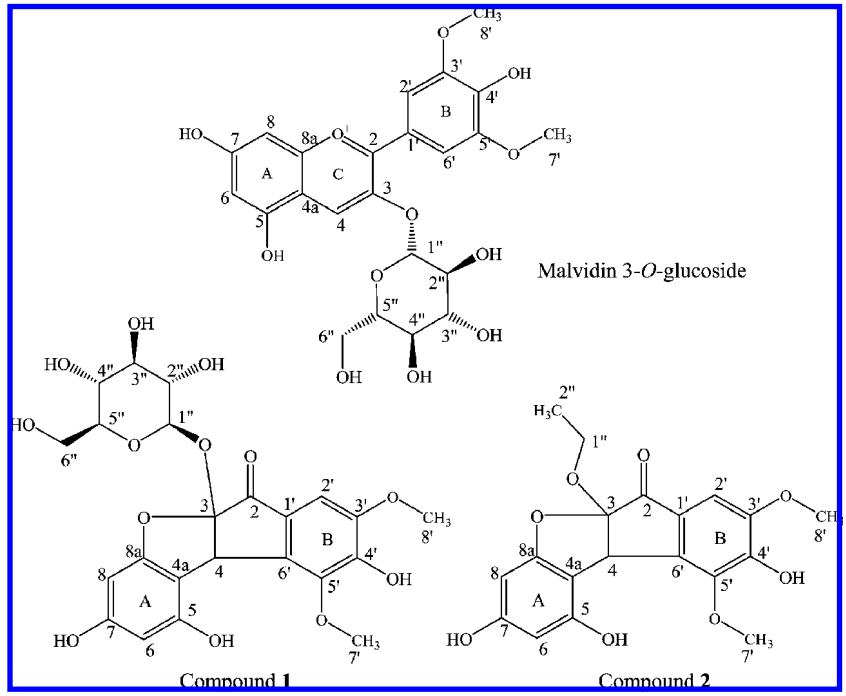

Figure 3. Structures of mavidin 3-*O*-glucoside and of the newly formed compounds **1** and **2**.

Table 2. ^{1}H and ^{13}C NMR Data of Compound **2** (DMSO-d_6/TFA)

position	δ ^{1}H (ppm), l, m, *J* (Hz)[a]	COSY	TOCSY	δ ^{13}C (ppm)[b]
4	4.78, 1, s		H-6, H-8	45.3
6	5.86, 1, d (1.8)	H-8	H-4, H-8	97.7
8	5.79, 1, d (1.8)	H-6	H-4, H-6	90.3
2′	7.02, 1, s			102.8
7′	3.91, 3, s			61.5
8′	3.81, 3, s			56.8
1″a	3.74, 1, dq (9.2, 7.1)	H-1″b, H-2″	H-1″b, H-2″	60.6
1″b	3.69, 1, dq (9.2, 7.1)	H-1″a, H-2″	H-1″a, H-2″	60.6
2″	1.10, 3, t (7.1)	H-1″a, H-1″b	H-1″a, H-1″b	15.7

[a] Values were recorded at 500 MHz. Integration: s, singlet; d, doublet; t, triplet; and dq, doublet quadruplet (*J* in Hz). [b] Assignments were based on a $^{1}H-^{13}C$ HMQC experiment.

substituent of this sp^3 carbon atom was deduced from the long-range HMBC correlations.

To get more information on the chemical structure of compound **1**, the chemical shifts of the quaternary carbons were attributed from the HMBC spectrum. From the observed correlations, a total of 23 carbon atom signals were deduced including six signals of the hexose moiety and two signals of the two methoxy groups. The other 15 carbon atoms correspond probably to the flavonoid skeleton, suggesting that the general C6−C3−C6 carbon chain was retained during the process.

The HMBC spectrum showed a cross-peak between the anomeric proton H-1″ (4.49 ppm) and the quaternary carbon located at 111.5 ppm, indicating that this carbon atom could be the aglycone carbon involved in the *O*-glucosidic bond. Keeping in mind the fact that the glucose moiety was linked to the C-3 carbon atom in the initial anthocyanin compound and taking into account the fact that it is very unlikely that the hexose could suffer any displacement during the reaction, the quaternary carbon atom located at 111.5 ppm was assumed to be C-3.

In the HMBC spectrum and in addition to their correlations with carbon signals located at 97.5 and 89.7 ppm and corresponding, respectively, to C-6 an C-8 attributed above, the two protons H-6 and H-8 showed correlations with four quaternary carbon atoms located at 160.3, 160.0, 154.7, and 103.7 ppm. From the low field chemical shift values, the first three signals were attributed to the oxygenated aromatic A ring carbons C-8a, C-7, and C-5, respectively, while the last signal located at 103.7 ppm was assigned to C-4a. Additional correlations between the H6/H8 protons and the sp^3 carbon atom located at 45.6 ppm, which is itself linked to the C-6′ carbon, were also observed. This suggests that the sp^3 carbon atom is in the 4-position.

In addition to its correlations with the carbons C-4a (103.7 ppm), C-5, and C-8 (154.7 and 160.3 ppm), the proton H-4 (5.27 ppm) attributed above showed cross-peaks with five other carbon atoms located at 139.8, 111.5, 123.5, 143.4, and 193.1 ppm. The first signal was concluded to be C-1′ from its chemical shift and also from its correlation with the residual B ring proton H-2′. The signal located at 143.4 ppm was attributed to the C-5′ from its correlation with the H-7′ and the signal at 123.5 ppm could be the carbon C-6′, which was concluded to be linked to the C-4 atom. The long-range correlation with the signal carbon atom located at 111.5 ppm assumed above to be the C-3 carbon confirmed this hypothesis. This carbon atom is in an α-position with the carbon 4 as attested by the correlation between the H-4 proton signal and the C-3 carbon signal. The carbon signal observed at 193.1 ppm could correspond to a benzylic carbonyl group concluded to be in the 2-position, in agreement with the HMBC correlations with H-4 and H-2′ protons.

These results require an oxidation step to yield compound **1** from malvidin glucoside. This oxidation is in agreement with the difference of 16 Da observed by MS analysis between the molecular mass of compound **1** and that of the initial anthocyanin, which is likely due to an hydration (+18 Da) followed by an oxidation process (−2 Da). This hypothesis is in agreement with the fact that the carbonyl group was concluded to be in the C-2 position, which constitutes the favorite position of water addition on anthocyanins.

The NMR analysis thus showed that compound **1** contains a sp^3 carbon atom, which was attributed to the C-4 carbon. This carbon was concluded to be linked to C-4a and C-6′ carbons from the HMBC correlations of its proton H-4 with the A ring (C-4a, C-5, and C-8a) and B ring (C-1′, C-3′, C-5′, and C-6′) carbons. The H-4 proton also showed a correlation with a

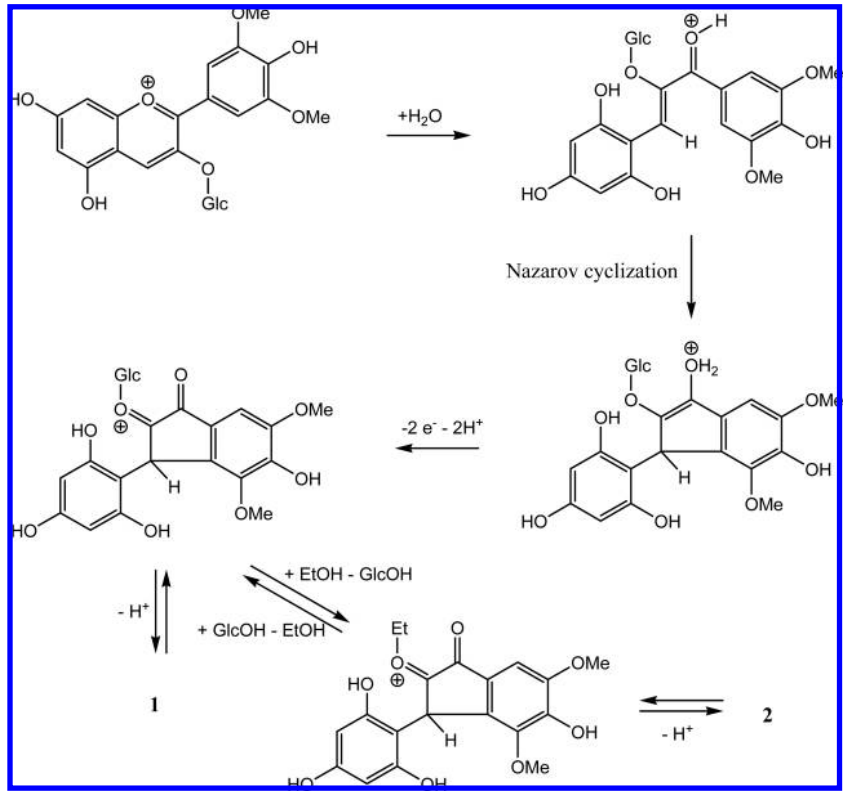

Figure 4. Hypothetical mechanism for the formation of compounds **1** and **2** from malvidin 3-*O*-glucoside in ethanolic medium.

quaternary carbon atom involved in the *O*-glucosidic linkage and concluded to be the C-3 carbon. Finally, a correlation was observed between H-4 and a benzylic carbon in the C-2 position as confirmed by the presence of a correlation between the C-2 and the B ring residual proton H-2′.

We could thus conclude that the initial malvidin A and B ring carbon−carbon linkages were not modified and that a first new five-membered ring was made during the reaction by linking the C-4 and C-6′ carbon atoms (**Figure 3**). A second five-membered ring was concluded to exist in the molecule structure by formation of an oxygenated linkage between C-3 and C-8a. The proposed structure $C_{23}H_{24}O_{13}$ is in agreement with the obtained NMR analysis (^{1}H, HMQC, and HMBC spectra) and the high-resolution MS analysis.

More information was also obtained from the ESI ion trap MS analysis where signals at *m*/*z* 531 and 1039 corresponding, respectively, to $[M + Na]^+$ and $[2M + Na]^+$ were observed. In addition, fragment ion signals at *m*/*z* 369 (−162 Da) and 351 (−180 Da) were also observed, corresponding to the loss of the anhydroglucose moiety and the loss of a glucose moiety. In the negative ion mode, a signal at *m*/*z* 507 corresponding to $[M - H]^-$ was observed. MS^2 fragmentation of this ion gave two major signals at *m*/*z* 345 $[M - H - 162]^-$ and *m*/*z* 327 $[M - H - 180]^-$, corresponding, respectively, to the loss of the anhydroglucose and the glucose moieties. MS^3 of the ion at *m*/*z* 327 produced two signals at *m*/*z* 312 and 297, corresponding, respectively, to the loss of one and two methyl groups. An extracted ion current chromatography recorded at *m*/*z* 507 (negative ion mode) or 531 (positive ion mode) showed the presence of another minor compound, which could be an isomer of compound **1**.

Structure Elucidation of Compound 2. The structural elucidation of compound **2** was initiated through ESI-MS analysis. The mass spectrum recorded in the negative ion mode showed signals at *m*/*z* 373 corresponding to the $[M - H]^-$ ion. Other fragments were observed at *m*/*z* 358 and 343 and corresponding to the loss of one and two methyl groups, respectively.

The ^{1}H NMR spectrum of compound **2** showed several similarities with that of compound **1**. Thus, the H-2′ singlet signal was observed at 7.02 ppm. The set of two doublets corresponding to the A ring H-6 and H-8 protons was observed at 5.86 and 5.79 ppm with a coupling constant of 1.8 Hz. The two methoxy protons signals appearing as singlets were observed at 3.91 (H-7′) and 3.81 ppm (H-8′), and the H-4 proton was observed as a singlet at 4.78 ppm.

Among the differences observed with the compound **1** ^{1}H NMR spectrum, we note the absence of the signals corresponding to the sugar moiety, indicating that the glucosyl group was missing in compound **2** and the presence of an additional ethoxy group. Thus, a signal integrating for three protons and appearing as a triplet ($J = 7.1$ Hz) was observed at 1.10 ppm. A set of two double quartets were observed at 3.74 ($J = 9.2$ and 7.1 Hz) and 3.69 ppm ($J = 9.2$ and 7.1 Hz) were observed. The presence of the ethoxy group was also confirmed through COSY correlations. The chemical shifts, the multiplicity, and the coupling constants of these signals are characteristics of an ethoxy group linked to an asymmetric carbon atom. The ethoxy group was thus concluded to be linked to the C-3 carbon atom. This may explain the low shielding (−0.5 ppm) observed in the chemical shift of the proton H-4 in compound **2** as compared to that of compound **1**. The structure proposed for compound **2** was thus similar to that of compound **1** with an ethoxy group instead of the glucose moiety (**Figure 3**). The other NMR spectroscopic data obtained for compound **2** gathered in **Table 2** were all in agreement with the proposed structure. In particular, the obtained ^{13}C NMR chemical shifts were in agreement with the presence of the ethoxy group.

Mechanism of Formation of Compounds 1 and 2. A mechanism of formation of the two newly formed compounds arising from malvidin 3-*O*-glucoside is presented in **Figure 4**. It may be noted that the proposed structure results from the

loss of two protons from the 2-hydrated malvidin compound. This form could exist either as hemiketal form or as two *cis*- and *trans*-chalcone forms, as discussed previously.

To explain a C−C bond formation between C-2′ and C-4, we have to advocate an opening of the C ring as a determinant step for this bond formation; therefore, the protonated chalcone form should be the first reaction intermediate through addition of water on malvidin glucoside. This protonated chalcone form may thereafter undergo a Nazarov-like cyclization, leading to an highly oxidizable 1,2-dihydroxy-cyclopentene ring, which is then oxidized, either because of the presence of residual oxygen in the solution or through dismutation with another reaction intermediate as postulated in a recent report (*37*). The vicinal keto oxonium system generated in this oxidation step can thereafter be attacked by a hydroxy group either intramolecularly from the phloroglucinol A ring or both intramolecularly and intermolecularly from ethanol, leading to compounds **1** or **2**, respectively.

In conclusion, in ethanolic solution, malvidin 3-*O*-glucoside was transformed to colorless compounds having absorption maxima between 295 and 300 nm. Two new molecules were isolated and structurally elucidated by NMR and MS. Both compound structures include 2−5 side rings through C−C and C−O−C linkages, respectively, between C-6′/C-4 and C-3/C-8a. Other compounds of unknown structure were also formed as shown in **Figure 2**. However, further research is still required, and the complete identification of other compounds from malvidin 3-*O*-glucoside degradation detected in this study should provide more information about the actual mechanism(s) involved in anthocyanin disappearance in model systems.

The structural characterization of these compounds provides important information regarding the chemical transformations involved in color changes during red wine aging. Indeed, the present work showed the formation of new compounds with original structures and through an original mechanism. It will be of interest to see if such or similar compounds are present in some fruit-derived foods and if the same mechanism could occur in foods and compete with other previously reported mechanisms. Taking into account the fact that food anthocyanins exist predominantly in their hydrated forms at food pH, the occurrence of such reactions during food processing and storage is very probable, especially if the process includes a heating step that favors the opening of the pyran ring (*1, 26*).

ACKNOWLEDGMENT

N. Es-Safi gratefully acknowledges the fellowship financial support from the International Foundation for Science (IFS).

Supporting Information Available: ^{1}H NMR spectra of compounds **1** and **2**. This material is available free of charge via the Internet at http://pubs.acs.org.

LITERATURE CITED

(1) Brouillard, R. Chemical structure of anthocyanins. In *Anthocyanins as Food Colors*; Markakis, P., Ed.; Academic Press, Inc.: New York, 1982; pp 1−38.

(2) Strack, D.; Wray, V. The anthocyanins. In *The Flavonoids: Advances in Research Since 1986*; Harborne, J. B., Ed.; Chapman & Hall: London, 1993; pp 1−22.

(3) Mercier, A.; Perdriel, G.; Rozier, J.; Cheraleraud, J. Note concerning the action of anthocyanin glycosides on the human electroretinogram. *Bull. Soc. Ophtalmol. Fr.* **1995**, *65*, 1049–1053.

(4) Matsumoto, H.; Nakamura, Y.; Tachibanaki, S.; Kawamura, S.; Hirayama, S. Stimulatory effect of cyanidin 3-glycosides on the regeneration of rhodopsin. *J. Agric. Food Chem.* **2003**, *51*, 3560–3563.

(5) Bomser, J.; Madhavi, D. L.; Singletary, K.; Smith, M. A. L. Anticancer activity of cranberry extracts. *Planta Med.* **1996**, *62*, 212–216.

(6) Katsube, N.; Iwashita, K.; Tsushida, T.; Yamaki, K.; Kobori, M. Induction of apoptosis in cancer cells by bilberry (*Vaccinium myrtillus*) and the anthocyanins. *J. Agric. Food Chem.* **2003**, *51*, 68–75.

(7) Hou, D. X. Potential mechanisms of cancer chemoprevention by anthocyanins. *Curr. Mod. Med.* **2003**, *3*, 149–159.

(8) Noda, Y.; Kaneyuki, T.; Igarashi, K.; Mori, A.; Packer, L. Antioxidant activity of nasunin, an anthocyanin in eggplant. *Res. Commun. Mol. Pathol. Pharmacol.* **1998**, *102*, 175–187.

(9) Noda, Y.; Kaneyuki, T.; Mori, A.; Packer, L. Antioxidant activities of pomegranate fruit extract and its anthocyanidins: Delphinidin, cyanidin, and pelargonidin. *J. Agric. Food Chem.* **2002**, *50*, 166–171.

(10) Tsuda, T.; Horio, F.; Osawa, T. Dietary cyanidin 3-*O*-beta-D-glucoside increases ex vivo oxidation resistance of serum in rats. *Lipids* **1998**, *33*, 583–588.

(11) Tsuda, T.; Horio, F.; Kitoh, J.; Osawa, T. Protective effects of dietary cyanidin 3-*O*-beta-D-glucoside on liver ischemia-reperfusion injury in rats. *Arch. Biochem. Biophys.* **1999**, *368*, 361–366.

(12) Tsuda, T.; Shiga, K.; Ohshima, K.; Kawakishi, S.; Osawa, T. Inhibition of lipid peroxidation and the active oxygen radical scavenging effect of anthocyanin pigments isolated from *Phaseolus vulgaris* L. *Biochem. Pharmacol.* **1996**, *52*, 1033–1039.

(13) Goto, T.; Kondo, T. Structure and molecular stacking of anthocyanins-flower color variation. *Angew. Chem., Int. Ed. Engl.* **1991**, *30*, 17–33.

(14) Daravingas, G.; Cain, R. F. Thermal degradation of black raspberry anthocyanin pigments in model systems. *J. Food Sci.* **1968**, *33*, 138–142.

(15) Adams, J. B. Thermal degradation of anthocyanins with particular reference to the 3-glycosides of cyanidin. I. In acidified aqueous solution at 100 °C. *J. Sci. Food Agric.* **1973**, *24*, 747–762.

(16) Iacobucci, G.; Sweeny, J. G. The chemistry of anthocyanins, anthocyanidins, and related flavylium salts. *Tetrahedron* **1983**, *39*, 3005–3038.

(17) Furtado, P.; Figueiredo, P.; Neves, H. C.; Pina, F. Photochemical and thermal degradation of anthocyanidins. *J. Photochem. Photobiol., A* **1993**, *75*, 113–118.

(18) Garcia-Viguera, C.; Bridle, P. Influence of structure on color stability of anthocyanins and flavylium salts with ascorbic acid. *Food Chem.* **1999**, *64*, 21–26.

(19) Cabrita, L.; Fossen, T.; Andersen, Ø. M. Colour and stability of the six common anthocyanidin 3-glucosides in aqueous solutions. *Food Chem.* **2000**, *68*, 101–107.

(20) Kirca, A.; Cemeroglu, B. Degradation kinetics of anthocyanins in blood orange juice and concentrate. *Food Chem.* **2003**, *81*, 583–587.

(21) Lopes, L.; Richard, T.; Saucier, C.; Teissedre, P. L.; Monti, J. P.; Glories, Y. Anthocyanone A: a quinone methide derivative resulting from malvidin 3-*O*-glucoside degradation. *J. Agric. Food Chem.* **2007**, *55*, 2698–2704.

(22) Tseng, K. C.; Chang, H. M.; Wu, J. S. B. Degradation kinetics of anthocyanin in ethanolic solutions. *J. Food Process. Preserv.* **2006**, *30*, 503–514.

(23) Brouillard, R.; Dubois, J. E. Mechanism of the structural transformation of anthocyanins in acid mediaj. *J. Am. Chem. Soc.* **1977**, *99*, 1359–1364.

(24) Brouillard, R.; Delaporte, B.; Dubois, J. E. Chemistry of the anthocyanin pigments. 2. Kinetic and thermodynamic study of proton transfer, hydration and tautomeric reactions of malvidin-3-glucoside. *J. Am. Chem. Soc.* **1977**, *99*, 8461–8468.

(25) Brouillard, R.; Lang, J. The hemiacetal-*cis*-chalcone equilibrium of malvin, a natural anthocyanin. *Can. J. Chem.* **1990**, *68*, 755–761.

(26) Brouillard, R.; Delaporte, B. Thermal degradation of anthocyanins. *Bull. Liaison-Groupe Polyphenols* **1978**, *8*, 205.

(27) Es-Safi, N.; Cheynier, V.; Moutounet, M. Role of aldehydic derivatives in the condensation of phenolic compounds with emphasis on the sensorial properties of fruit-derived foods. *J. Agric. Food Chem.* **2002**, *50*, 5571–5585.
(28) Es-Safi, N.; Le Guernevé, C.; Fulcrand, H.; Cheynier, V.; Moutounet, M. New polyphenolic compounds with xanthylium skeletons formed through reaction between (+)-catechin and glyoxylic acid. *J. Agric. Food Chem.* **1999**, *47*, 5211–5217.
(29) Es-Safi, N.; Le Guernevé, C.; Labarbe, B.; Cheynier, V.; Moutounet, M. Structure of a new xanthylium salt derivative. *Tetrahedron Lett.* **1999**, *40*, 5869–5872.
(30) Remy-Tanneau, S.; Le Guernevé, C.; Meudec, E.; Cheynier, V. Characterisation of a colorless anthocyanin-flavan-3-ol dimer containing both carbon-carbon and ether interflavanoid linkages by NMR and mass spectrometry. *J. Agric. Food Chem.* **2003**, *51*, 3592–3597.
(31) Sarni-Manchado, P.; Cheynier, V.; Moutounet, M. Reactions of polyphenoloxidase generated caftaric acid *o*-quinone with malvidin 3-*O*-glucoside. *Phytochemistry* **1996**, *45*, 1365–1369.
(32) Santos-Buelga, C.; Bravo-Haro, C.; Rivas-Gonzalo, J. C. Interactions between catechin and malvidin-3-monoglucoside in model solutions. *Lebensm.-Unters. Forsch.* **1995**, *201*, 269–274.
(33) Fulcrand, H.; Cameira dos Santos, P.; Sarni-Manchado, P.; Cheynier, V.; Favre-Bonvin, J. Structure of new anthocyanin-derived wine pigments. *J. Chem. Soc., Perkin Trans. 1* **1996**, 735–739.
(34) Bakker, J.; Timberlake, C. F. Isolation, identification, and characterization of new color-stable anthocyanins occurring in some red wines. *J. Agric. Food Chem.* **1997**, *45*, 35–43.
(35) Sarni, P.; Fulcrand, H.; Souillol, V.; Souquet, J. M.; Cheynier, V. Mechanisms of anthocyanin degradation in grape must-like model solutions. *J. Sci. Food Agric.* **1995**, *69*, 385–391.
(36) Panichpol, K.; Waterman, P. G. Novel flavonoids from the stem of *Popowia cauliflora*. *Phytochemistry* **1978**, *17*, 1363–1373.
(37) Ghidouche, S.; Es-Safi, N.-E.; Ducrot, P.-H. Mechanistic study on the enzymatic oxidation of flavonols. *Tetrahedron Lett.* **2008**, *49*, 619–623.

Received for review January 18, 2008. Revised manuscript received March 31, 2008. Accepted April 1, 2008.

JF8001872